

CALCULATION OF THE AGS OPTICS BASED ON 3D FIELDS DERIVED FROM EXPERIMENTALLY MEASURED FIELDS ON MEDIAN PLANE*

N. Tsoupas[†], J. S. Berg, S. Brooks, F. Méot, V. Ptitsyn, D. Trbojevic
 Brookhaven National Laboratory, Upton, NY, USA

Abstract

Closed orbit calculations of the Alternating Gradient Synchrotron (AGS) were performed and the beam parameters at the Fast Beam Extraction (FEB) point of the AGS [1] were calculated using a modified RAYTRACE computer code [2] to generate 3D fields from measured field maps on the median plane of the AGS combined function magnets. The algorithm which generates 3D fields from field maps on a plane is described in reference [3] which discusses the details of the mathematical foundation of this approach. In this paper we discuss results from studies reported in Refs. [1,4] that are based on the 3D fields generated from measured field components on a rectangular grid of a plane. A brief overview of the algorithm used will be given, and one of the two methods of calculating the required field derivatives on the plane will be discussed.

INTRODUCTION

The AGS is one of the pre-acceleration stages of the RHIC complex. Figure 1 is an aerial picture of the site with the green trace indicating the tunnel of the AGS. The 240 com-

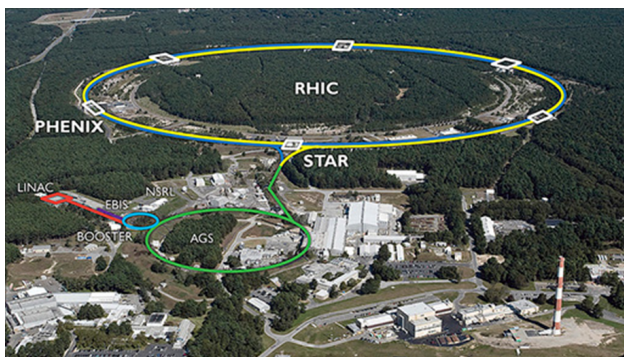


Figure 1: Area view of the RHIC complex. The green trace indicates the location of the AGS tunnel.

combined function main magnets of the AGS are placed inside the AGS tunnel whose schematic diagram is showing in Fig. 2. The AGS main magnets are separated in 12 superperiods of 20 magnets per superperiod spanning an arc of 30° as shown in Fig. 2.

Figure 3 is a schematic diagram of the main magnets layout (small rectangles) in each superperiod. The “+” and “-” signs on each magnets indicate the focusing and defocusing quadrupole property of each combined function magnet for positive ions circulating in the synchrotron.

* Work supported by the US Department of Energy
[†] tsoupas@bnl.gov

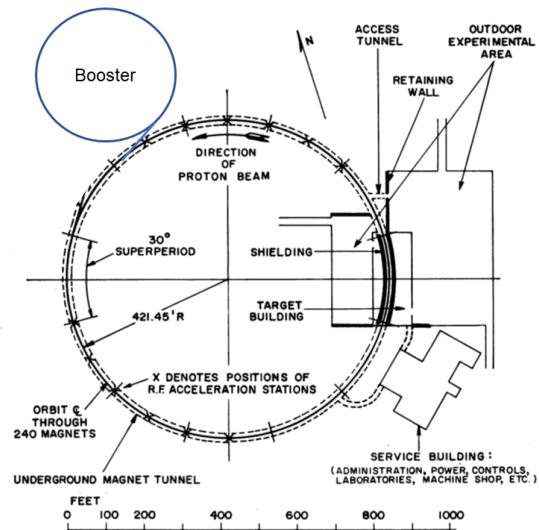


Figure 2: Schematic diagram of the AGS tunnel. The 240 main AGS magnets are separated in 12 superperiods with 20 magnets per superperiod which spans an arc of 30°

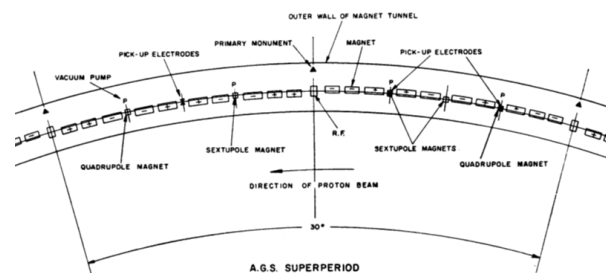


Figure 3: Drawing of the AGS superperiod which consists of 20 combined function main magnets. The “+” and “-” signs on each magnet indicate the focusing and defocusing quadrupole property of each combined function magnet for positive ions circulating in the synchrotron. There is one tune quadrupole in each of the straight sections SS03, SS17 and one chromaticity sextupole in each of the straight sections SS07, SS13 of each superperiod.

There is one tune quadrupole in each of the straight sections SS03, SS17 and one chromaticity sextupole in each of the straight sections SS07, SS13 of each superperiod. Three pickup electrodes are also located in the straight sections SS03, SS05, and SS13 respectively. Additional information on the AGS appears in Refs. [1, 5].

BEAM OPTICS OF AGS

The beam optics of the AGS for a charged particle beam which is not subject to space charge forces depends on the

Content from this work may be used under the terms of the CC BY 3.0 licence (© 2018). Any distribution of this work must maintain attribution to the author(s), title of the work, publisher, and DOI.

magnetic field of the magnetic elements of the AGS ring. These fields can be either calculated using various methods, or can be measured. In this study we make use of the measured magnetic fields of the AGS combined function magnets. These fields were measured on a grid located on the median plane of the combined function magnets as it is described in one of the following sections. In the next section we introduce the reader to the AGS main magnets.

The AGS Combined Function Magnets

The 240 AGS main magnets are made of three type of magnets named A, B, and C. Magnets type A and B have the same cross section and lengths 90" and 75" respectively, and magnet C has a length of 90". The table in Fig. 4 lists the lengths of the three type of magnets and shows pictures of their cross sections. By rotating the magnets A, B, C, by 180° about the vertical axis the focusing property of the magnets changes from focusing to defocusing.

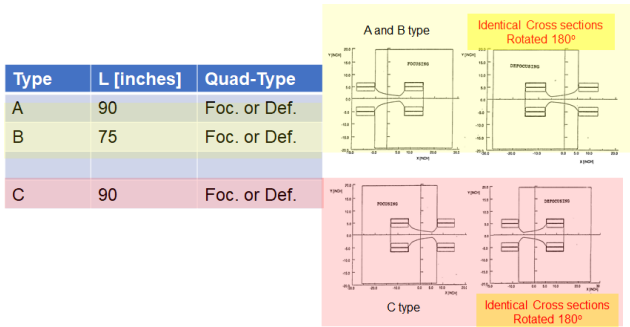


Figure 4: The three types A, B, and C of the AGS combined function magnets. Magnets type A and B have the same cross section but different lengths. By rotating the magnets by 180° about the vertical axis the focusing property of the magnets changes from focusing to defocusing.

Figure 5 is a picture of a C-type AGS combined function magnet.

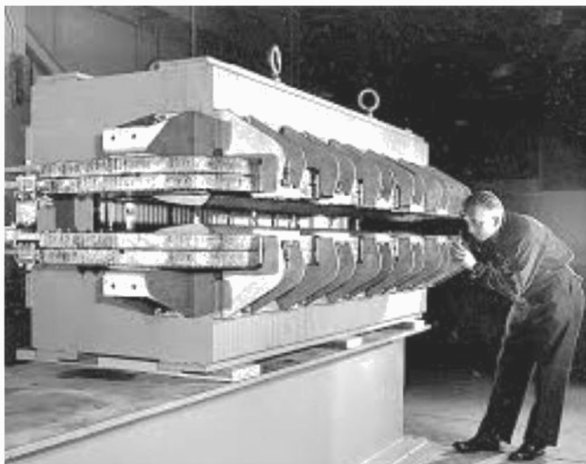


Figure 5: A picture of a C-type AGS combined function magnet.

The Field Maps of the AGS Main Magnets

The field map of a single type A and a single type C magnet were measured on the median plane of each magnet. Figure 6 is a top view of the magnets showing the areas (ABCD) and (EFGH) over which the field maps of magnet type A were performed (picture on the left) and the area (ABCD) over which the field maps of magnet type C was performed (picture on the right). For magnet type A (left

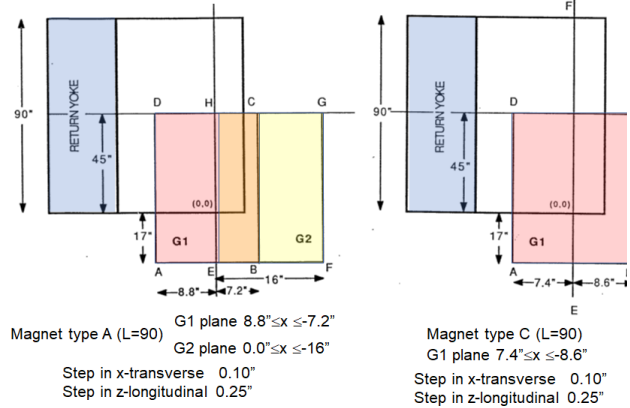


Figure 6: Top view of magnets type A (left) and C (right). The dimensions of the areas G1 (ABCD) and G2 (EFGH) over which the field maps were performed on each magnet appear in the figure.

picture in Fig. 6) two field maps were measured, the G1 over the area (ABCD) and G2 over the area (EFGH). The rectangular grid size of each field map was 0.1" in the transverse x-direction and 0.25" in the longitudinal z-direction. For magnet type C (right picture in Fig. 6) one field map G1 over the area (ABCD) was measured with a rectangular grid size of 0.1" in the transverse x-direction and 0.25" in the longitudinal z-direction. The dimensions of the areas over which the field maps were measured appear on Fig. 6. Although these field maps cover only half of the magnet's median plane, the symmetry of the magnet was used to complete the field map over the entire area of the magnet's median plane.

Brief Description of the Algorithm

This section provides a brief description of the algorithm which is used in the RAYTRACE code [2] to calculate the field components of the AGS main magnets from the measured field maps on the median plane of the magnet.

Figure 7 shows the grid points (intersection points of the red lines) on a plane where the magnetic field components (yellow arrows) are measured. The algorithm calculates the magnetic field components (blue arrows) at any given point in space at a distance y from the plane. The algorithm is based on the Taylor series expansion of the magnetic field components at a point located at a distance y from the plane in terms of the y coordinate. This expansion is shown in Eq. (1).

$$B_i(x, y, z) = \sum_{j=0}^4 \frac{1}{j!} \frac{\partial^j B_i(x, y, z)}{\partial y^j} \Big|_{y=0} y^j = \sum_{j=0}^4 a_{ij}(x, z) y^j \quad (1)$$

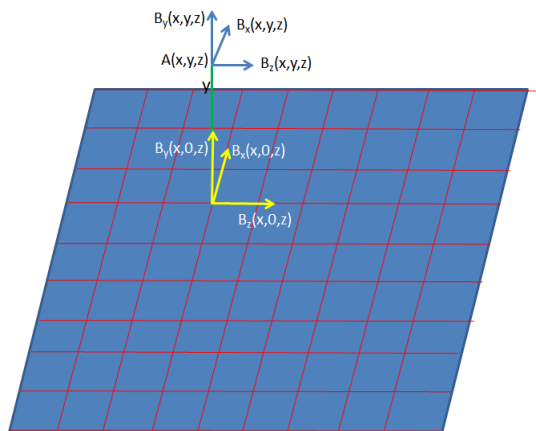


Figure 7: A schematic diagram of a grid on a plane. The magnetic field components (yellow arrows) at any grid point on the plane are measured. The algorithm calculates the magnetic field components (blue arrows) at any given point in space at a distance y from the plane.

Since the values of the field components on the plane ($y=0$) are known the task is to express the coefficients of expansion $a_{ij}(x, z)$ in terms of these field components on the plane and also in terms of their partial derivatives of these field components with respect to the x and z spatial coordinates. This is done by constraining the magnetic fields of Eq. (1) to satisfy the Maxwell's equations:

$$\vec{\nabla} \cdot \vec{B}(x, y, z) = 0 \quad \text{and} \quad \vec{\nabla} \times \vec{B}(x, y, z) = 0 \quad (2)$$

In **APPENDIX I** the coefficients a_{ij} are expressed in term of the known measured field components on the plane and their spatial derivatives with respect to x and z .

Reference [6] provides a detailed derivation of the coefficients a_{ij} in terms of the measured fields on the plane and their partial spatial derivatives.

CLOSED ORBIT CALCULATIONS AND BEAM EXTRACTION

This section describes the procedure that was used to extract the beam bunches from the AGS and report the results of the beam optics just before and during the fast beam extraction process from the AGS. All the calculations are based on the numerical integration of the equation of motion of particles moving in the magnetic field which was derived from the experimentally measured field maps using the algorithm mentioned earlier. The RAYTRACE code was employed to calculate the fields and integrate the equation of motion of the particles in the AGS [1]. At the extraction energy and prior to the beam extraction two local beam bumps are generated in the AGS. One of the local beam bumps brings the beam inside the “G10” extraction kicker and the second local beam bump brings the beam close to the “H10” extraction septum. The green trace in Fig. 8 is the closed orbit in the AGS prior to fast beam extraction. The local “G10” and “H10” beam bumps are shown as part of the green trace. The

red trace corresponds to trajectory of the extracted beam. Details on the formation of the local extraction beam bumps “G10” and “H10” appear in Ref. [1].

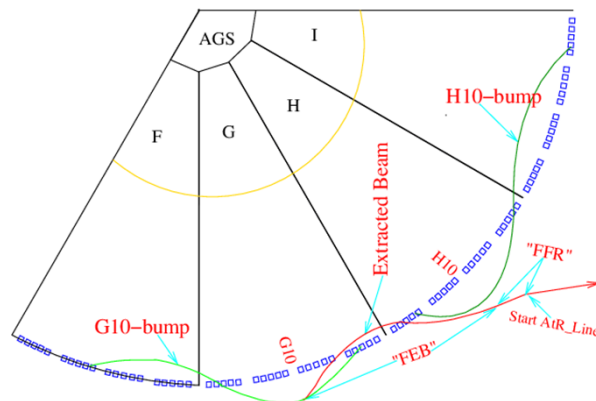


Figure 8: A schematic diagram of a section of the AGS. The green trace is the closed orbit in the AGS prior to fast beam extraction. The local “G10” and “H10” beam bumps are shown as part of the green trace. The red trace corresponds to trajectory of the extracted beam.

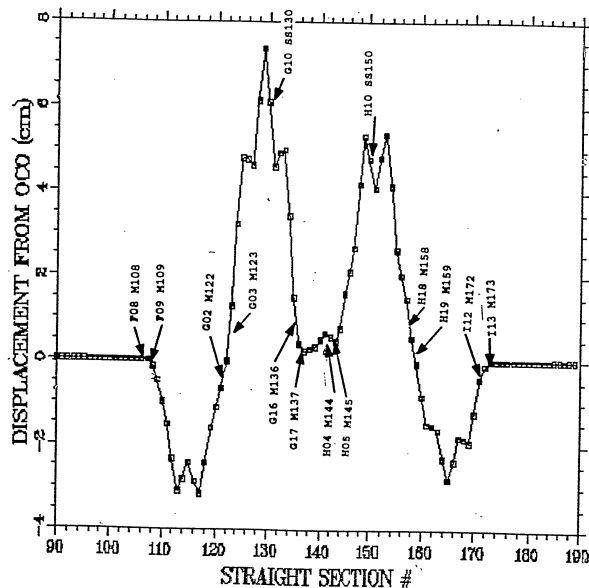


Figure 9: Displacement of the closed orbit in the straight sections starting from (SS90) and ending at (SS190). Both the local beam bumps G10 and H10 are on. The label at the beginning of each small arrow is the name of the combined function magnet.

Figure 9 shows the beam displacement at the middle of the straight sections of the AGS when the closed orbit extraction bumps “G10” and “H10” are excited. The label at the beginning of the small arrow corresponds to the name of the combined function magnet.

Figure 10 shows the horizontal β_x (left) and β_y (right) functions of the closed orbit at the middle of the straight sections with the extraction bumps “G10” and “H10” on.

Content from this work may be used under the terms of the CC BY 3.0 licence (© 2018). Any distribution of this work must maintain attribution to the author(s), title of the work, publisher, and DOI.

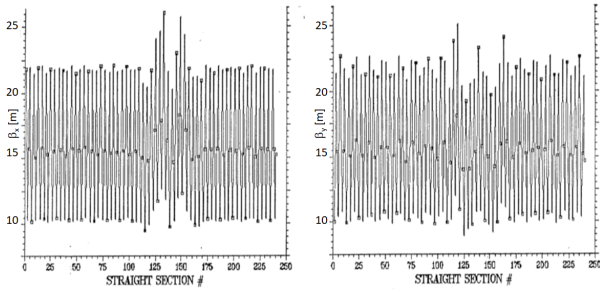


Figure 10: The β_x (left) and β_y (right) functions at the middle of the straight sections of the AGS with the extraction bumps “G10” and “H10” on. The line is to guide the eye.

Figure 11 shows the horizontal η_x function of the closed orbit at the middle of the straight sections with the extraction bumps “G10” and “H10” on.

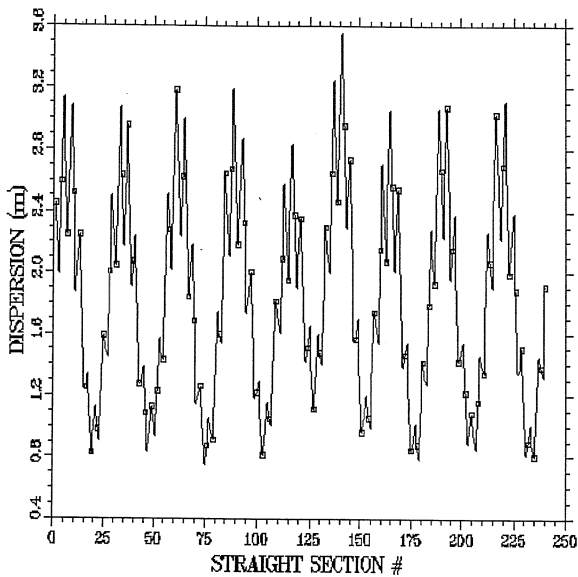


Figure 11: The horizontal η_x function at the middle of the straight sections of the AGS with the extraction bumps “G10” and “H10” on. The line is to guide the eye.

THE FAST BEAM EXTRACTION

Upon the formation of the closed orbit in AGS with the local “G10” and “H10” beam bumps on as described in the previous section, the bunched beam can be extracted from the AGS by energizing the G10 fast kicker which generates a magnetic field pulse of duration ~ 200 nsec and provides a kick to the beam of 1.5 mrad. The location of the G10 kicker is shown in Fig. 12 and the red trace initiating from the G10 kicker represents the extracted beam which is displaced at the location of the H10 septum by ~ 6 cm to enter in the main field region of the H10 septum which deflects the beam by ~ 20 mrad to extract it from the AGS. The table in Fig. 12 shows the R-matrix elements between the location of the G10 kicker and the start of the AGS-to-RHIC (AtR) transfer line shown in Fig. 12. The AtR line is the beam transfer line

from the AGS to the Relativistic Heavy Ion Collider (RHIC). The knowledge of this R-matrix and the knowledge of the beta and eta functions from the closed orbit calculations at the location of the G10 kicker provide the values of the beta and eta functions at the beginning of the AtR line as shown by the matrix equations at the bottom of Fig. 12. Again the R-matrix from the location of the G10 kicker to the beginning of the AtR line was calculated by raytracing many rays in the magnetic field which was computed from the measured field maps using the algorithm mentioned earlier.

R Matrix G10-kicker to Start-AtR					
-1.8261	-17.443	0.0	0.0	0.0	-2.5889
0.17912	1.1634	0.0	0.0	0.0	0.2517
0.0	0.0	1.125	-15.016	0.0	0.0
0.0	0.0	0.186	-1.5855	0.0	0.0
-0.0041	1.3785	0.0	0.0	1	0.0
0.0	0.0	0.0	0.0	0.0	1.0

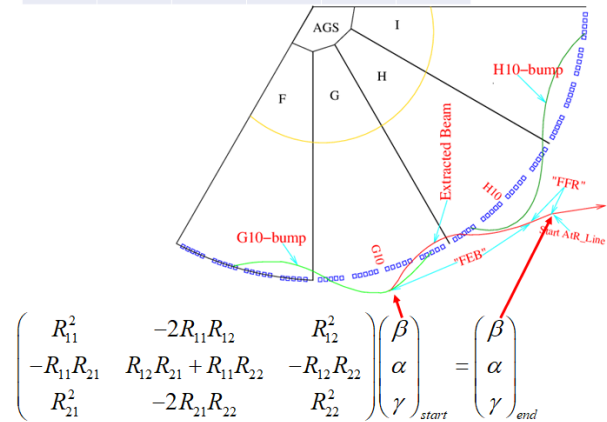


Figure 12: The red trace initiating from the location of the G10 kicker represents the trajectory of the reference orbit of the extracted beam. The table on top of the figure is the R-matrix between the location of the G10 kicker and the beginning of the AtR line.

CONCLUSION

From measured field maps at the median plane of the AGS combined function main magnets, the magnetic fields in circulating beam region were calculated by the use of an algorithm discussed in this paper. From these fields the beam parameters ($\beta_{x,y}$ and $\eta_{x,y}$) of the closed orbit of the circulating beam in AGS beam were calculated. Subsequently the extraction kicker “G10” of the AGS was energized and the beam was extracted from the AGS. Using the magnetic fields along the extraction channel the R-matrix elements from the location of the G10 kicker to the beginning of the AtR line were calculated and therefore the beam parameters at the beginning of the AtR line were calculated.

APPENDIX I

Expression of the coefficients a_{ij} Applying Maxwell’s Equations (2) on the magnetic field which is given by Equation (1) the following expressions of the coefficients a_{ij} are derived.

The 0th order a_{i0} coefficients

$$a_{x0} = B_x(x, 0, z), a_{y0} = B_y(x, 0, z), a_{z0} = B_z(x, 0, z) \quad (3)$$

The 1st order a_{i1} coefficients

$$a_{x1} = \frac{\partial B_y(x, 0, z)}{\partial x} \quad (4)$$

$$a_{y1}(x, z) = - \left(\frac{\partial B_x(x, 0, z)}{\partial x} + \frac{\partial B_z(x, 0, z)}{\partial z} \right) \quad (5)$$

$$a_{z1} = \frac{\partial B_y(x, 0, z)}{\partial z} \quad (6)$$

The 2nd order a_{i2} coefficients

$$a_{x2} = -\frac{1}{2} \left(\frac{\partial^2 B_x(x, 0, z)}{\partial x^2} + \frac{\partial^2 B_z(x, 0, z)}{\partial x \partial z} \right) \quad (7)$$

$$a_{y2} = -\frac{1}{2} \left(\frac{\partial^2 B_y(x, 0, z)}{\partial x^2} + \frac{\partial^2 B_y(x, 0, z)}{\partial z^2} \right) \quad (8)$$

$$a_{z2} = -\frac{1}{2} \left(\frac{\partial^2 B_x(x, 0, z)}{\partial z \partial x} + \frac{\partial^2 B_z(x, 0, z)}{\partial z^2} \right) \quad (9)$$

The 3rd order a_{i3} coefficients

$$a_{x3} = -\frac{1}{6} \left(\frac{\partial^3 B_y(x, 0, z)}{\partial x^3} + \frac{\partial^3 B_y(x, 0, z)}{\partial x \partial z^2} \right) \quad (10)$$

$$a_{y3} = \frac{1}{6} \left(\frac{\partial^3 B_x(x, 0, z)}{\partial x^3} + \frac{\partial^3 B_z(x, 0, z)}{\partial x^2 \partial z} + \frac{\partial^3 B_x(x, 0, z)}{\partial z^2 \partial x} + \frac{\partial^3 B_z(x, 0, z)}{\partial z^3} \right)$$

$$a_{z3} = -\frac{1}{6} \left(\frac{\partial^3 B_y(x, 0, z)}{\partial z \partial x^2} + \frac{\partial^3 B_y(x, 0, z)}{\partial z^3} \right) \quad (11)$$

The 4th order a_{i4} coefficients

$$a_{x4} = \frac{1}{24} \left(\frac{\partial^4 B_x(x, 0, z)}{\partial x^4} + \frac{\partial^4 B_z(x, 0, z)}{\partial x^3 \partial z} + \frac{\partial^4 B_x(x, 0, z)}{\partial x^2 \partial z^2} + \frac{\partial^4 B_z(x, 0, z)}{\partial x \partial z^3} \right) \quad (12)$$

$$a_{y4} = -\frac{1}{24} \left(\frac{\partial^4 B_y(x, 0, z)}{\partial x^4} + 2 \frac{\partial^4 B_y(x, 0, z)}{\partial x^2 \partial z^2} + \frac{\partial^4 B_y(x, 0, z)}{\partial z^4} \right) \quad (13)$$

$$a_{z4} = \frac{1}{24} \left(\frac{\partial^4 B_x(x, 0, z)}{\partial z \partial x^3} + \frac{\partial^4 B_z(x, 0, z)}{\partial x^2 \partial z^2} + \frac{\partial^4 B_x(x, 0, z)}{\partial z^3 \partial x} + \frac{\partial^4 B_z(x, 0, z)}{\partial z^4} \right) \quad (14)$$

Calculation of the Partial Field Derivatives

The partial derivatives of the field components appearing in the expression of the coefficients a_{ij} can be calculated either numerically or using the “fit a function method” which is the method used in the studies discussed in Refs. [1, 4]. Both methods are discussed in details in Ref. [6].

Fit a Function method Figure 13 shows the grid points of the global (x, z) coordinate system where the field components $[B_x(x, y = 0, z), B_y(x, y = 0, z), B_z(x, y = 0, z)]$ are measured, and also shows two of the many “small-grid-areas” (ABCD), (EFGH) in which the global grid is partitioned.

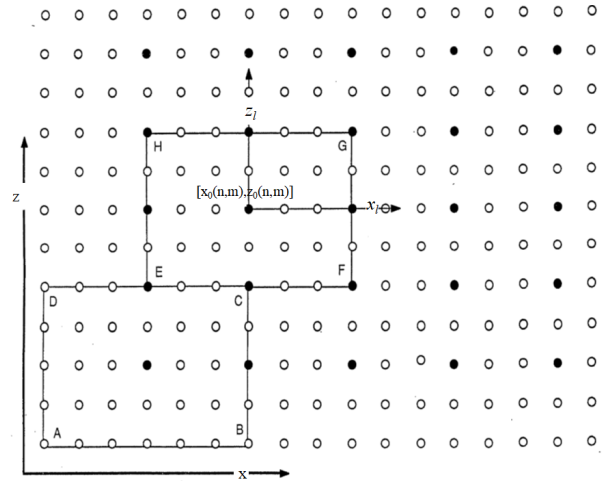


Figure 13: The large 2D grid in the (x, z) coordinate system is partitioned in many “small-grid-areas” two of these small areas (ABCD), (EFGH) are shown. The small grid areas may overlap, and each area can be characterized by the (n, m) indices and its local (x_l, y_l) coordinate system. The local coordinates (x_l, y_l) of each small grid are related to the global (x, z) coordinates through the equations $x = x_0(n, m) + x_l$ and $z = z_0(n, m) + z_l$.

The small grid areas may partially overlap with each other, and each area can be characterized by the (n, m) indices and its associated (x_l, y_l) local coordinate system. With this method a polynomial function shown in Eq. (15), is fitted to the experimentally measured values of the magnetic field components. The local coordinates (x_l, y_l) of each small grid are related to the global coordinates (x, z) through the equations $x = x_0(n, m) + x_l$ and $z = z_0(n, m) + z_l$, where $x_0(n, m)$ and $z_0(n, m)$ are the global coordinates of the centers $(x_l, y_l) = (0, 0)$ of the “small-grid-area” which is characterized by the indices (n, m) .

$$B_i(n, m, x_l, z_l) = \sum_{j=0}^4 \sum_{k=0}^4 c_{i, n, m, j, k} (x_l)^j (z_l)^k \quad (15)$$

In Eq. (15) the index i corresponds to the field component with $i = (1, 2, 3) \Leftrightarrow (x, y, z)$ and the indices n, m correspond to the particular “small-grid-area” of the global grid. The x_l, z_l variables are the local coordinates of this “small-grid-area”

which are related to the global coordinates (x, z) through equations mentioned earlier. The coefficients $c_{i,n,m,j,k}$ are calculated using the method of Singular Value Decomposition (SVD) [7] which is applied to solve N equations with M unknowns ($N \geq M$). This method of fitting a function to the experimentally measured field components at the grid points of a rectangular grid on the median plane of a magnet has been used in the RAYTRACE code to calculate the beam optics of the AGS synchrotron [1] using the median plane field maps of the AGS combined function magnets.

REFERENCES

- [1] N. Tsoupas *et al.*, “Closed orbit calculations at AGS and Extraction Beam Parameters at H13,” AD/RHIC/RD-75, Oct. 1994.
- [2] S. B. Kowalski and H. A. Enge, “The Ion-Optical Program Raytrace,” *NIM A*, vol. 258, pp. 407, 1987.
- [3] K. Makino, M. Berz, and C. Johnstone, “High-Order Out-Of-Plane Expansion for 3D Fields,” *Int. Journal of Modern Physics A*, vol. 26, pp. 1807-1821, 2011.
- [4] N. Tsoupas *et al.*, “Effects of Dipole Magnet Inhomogeneity on the Beam Ellipsoid,” *NIM A*, vol. 258, pp. 421-425, 1987.
- [5] “Alternating Gradient Synchrotron Project Construction Completion Report,” CAD report BNL 1966
- [6] N. Tsoupas *et al.*, “Algorithm to calculate off-plane magnetic field from an on-plane field map,” C-A/AP/605, May 2018.
- [7] W. H. Press *et al.*, “Singular Value Decomposition”, in *Numerical Recipes. The Art of Scientific Computing*. Cambridge University Press, MA, USA.